

# Poly(vinyl-pyrrolidone) assisted hydrothermal synthesis of flower-like CdS nanorings

Guojun Song · Hui Zhang · Jianjiang Li · Zhi Peng · Xiaoru Li · Lina Chen

Received: 3 October 2011 / Revised: 11 January 2012 / Accepted: 12 February 2012 /  
Published online: 19 February 2012  
© Springer-Verlag 2012

**Abstract** Well-defined CdS nanorings with flower-like morphology were synthesized by a hydrothermal method using poly(vinyl-pyrrolidone) as capping agent. The phase composition, morphology, structure, and optical properties of CdS nanorings were characterized by X-ray diffraction (XRD), scanning electron microscope, transmission electron microscopy, and UV–vis absorption spectroscopic techniques. The XRD pattern of the sample can be indexed to the cubic zinc blende phase CdS. According to the quantitative analysis of energy-dispersive spectrum, the Cd:S molar ratio of the sample is about 1:0.96. The possible formation mechanism of the CdS nanorings is proposed which is based on time-resolved experiments. Furthermore, the absorption peak of CdS nanorings is red-shifted to 523 nm in the UV–vis absorption spectrum.

**Keywords** CdS nanorings · Flower-like · Hydrothermal method · Formation mechanism

## Introduction

Nanoscale semiconductor crystals with controlled size and shape have attracted intensive research interests, owing to their novel properties and potential applications in optics, electronics, catalysis, magnetism, and biology [1]. In recent years, syntheses of more complex three-dimensional (3D) architectures have been extensively investigated because studies on these complex structures are useful to understand their formation mechanism and fabricate electronic or photonic nanodevices [2].

CdS, which is one of the most classical direct band gap II–VI semiconductors [3, 4], is now widely used in light-emitting diodes, photocatalyst, solar cell, single

G. Song (✉) · H. Zhang · J. Li · Z. Peng · X. Li · L. Chen  
Institute of Polymer Materials, Qingdao University, Qingdao 266071, China  
e-mail: doudoulingdao@126.com

charge memories, luminescent nanocomposites, and diagnostic agents in medicine [5–10]. Over the past few years, much effort has been paid on the fabrication of CdS with specialized size and morphology [11, 12]. And many methods have been developed to fabricate CdS with novel morphologies. Fan et al. [13] have synthesized large-scale 3D CdS spheres composed of hexagon-based pyramids through a facile solution-phase reaction. Dongre et al. [14] have synthesized flower-like CdS nanostructures through chemical bath deposition and wet chemical etching method. Nan et al. [15] have synthesized well-defined intersectional CdS nanocrystalline thin films with a conifer-like morphology by a facile electrochemical process. Chen et al. [16] have synthesized large-scale 3D CdS nanocrystals with a flower-like morphology through hydrothermal treatment in water free from organic solvents and surfactants. Xiong et al. [17] have reported a facile L-cysteine and ethanolamine (EA)-synergistically assisted hydrothermal route to synthesize various self-assembled CdS nanostructures including water lily-like nanocrystals, rice-like nanorods, nanofans by nanorod bunches, urchin microflowers, and porous microparticles. Although different methods have been used to synthesize CdS nanocrystals with various shapes, synthesis of CdS nanorings by a solution-based route is rarely reported. Therefore, it is imperative and desirable to develop solution-based methods to prepare novel CdS nanorings.

In this article, well-defined CdS nanorings with flower-like morphology were synthesized by hydrothermal reaction of cadmium nitrate tetrahydrate ( $\text{Cd}(\text{NO}_3)_2 \cdot 4\text{H}_2\text{O}$ ) and thioacetamide (TAA) with poly(vinyl-pyrrolidone) (PVP) as capping agent. The morphology of the product differed from those reported in previous researches. The possible growth mechanism of the CdS nanorings was also proposed on the base of the characterization of their crystal structures and the morphology analysis.

## Experimental section

### Materials and preparation

All of the reactants and solvents are analytical-grade and used without any further purification. In a typical procedure, 1.5 mmol  $\text{Cd}(\text{NO}_3)_2 \cdot 4\text{H}_2\text{O}$  and 1.00 g of PVP were dissolved in 30 mL of distilled water with magnetic stirring at room temperature for 30 min to obtain a uniform solution. After that, 1.8 mmol of TAA was added to the solution and kept stirring for another 30 min, and then the mixture was transferred into a 50-mL Teflon-lined autoclave. The autoclave temperature was maintained at 180 °C for 8 h. After the mixture cooled to room temperature naturally, the yellow precipitate was washed with distilled water and ethanol for several times. The final product was dried in a vacuum oven at 60 °C for 6 h.

### Characterization

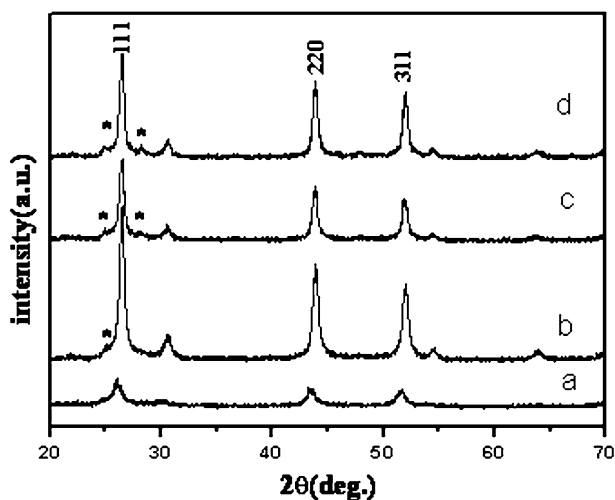
Powder X-ray diffraction (XRD) was used to determine the crystalline phases on a Rigaku D/Max2200VPC X-ray diffractometer (Cu  $K\alpha$  radiation,  $\lambda = 1.5406 \text{ \AA}$ ).

Scanning electron microscope (SEM) was used to image the morphology of nanorings on a JEOL JSM-6390LV SEM. An energy-dispersive spectrum (EDS) on a JEOL JSM-6390LV SEM was used to conduct element analysis. Transmission electron microscopy (TEM) characterization was performed on a JEOL JEM-2100 FEG TEM. UV–vis absorption spectrum was measured on a TU-1810DPC UV–vis spectrophotometer.

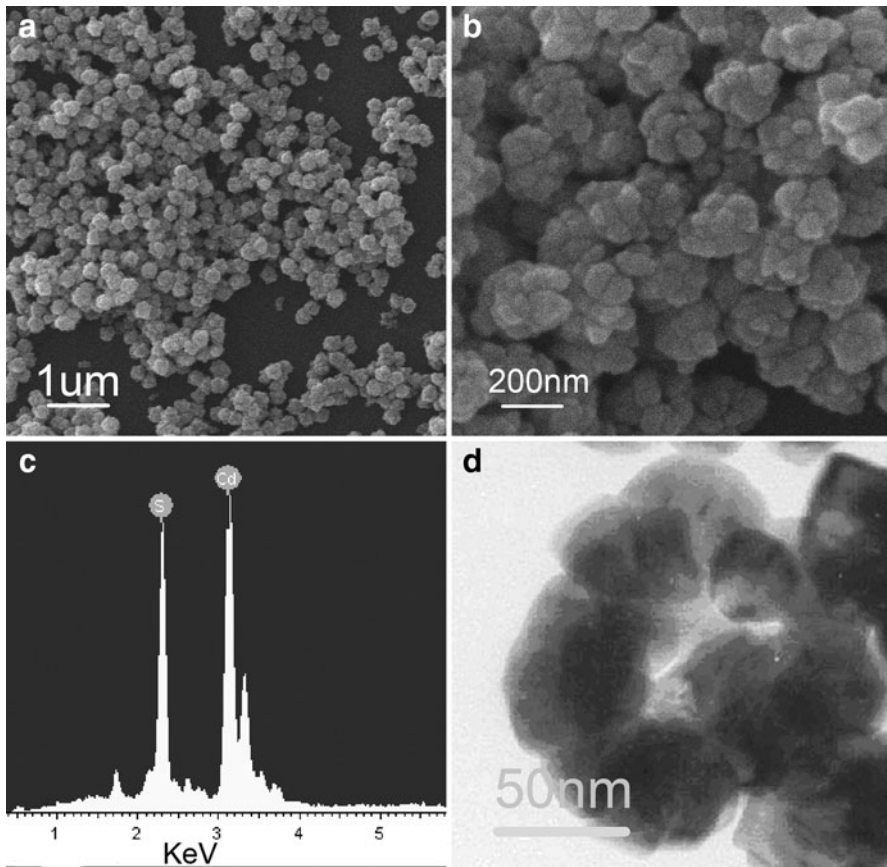
## Results and discussion

Figure 1 displays the XRD patterns of as-synthesized products for different reaction time. The XRD patterns of all samples can be consistently indexed to the cubic zinc blende phase CdS, in which the several prominent peaks correspond to the reflection (111), (220), and (311) [18]. As the reaction time increased, the crystallinity of the samples continuously improved as indicated by stronger and narrower XRD peaks. The broadening of peaks in Fig. 1a indicates the small sizes of CdS nanocrystals. However, the appearance of  $2\theta = 24.8^\circ$  and  $28.1^\circ$  peaks with increasing reaction time indicates the formation of the hexagonal CdS phase. That is to say, cubic CdS nanocrystals were obtained at the initial growth stage, and hexagonal CdS nanocrystals were formed with increasing reaction time. The possible reason is that the cubic structure of CdS nanocrystals is a nonequilibrium and metastable phase [19].

Figure 2 shows the typical SEM, EDS, and TEM images of the sample prepared at  $180^\circ\text{C}$  for 8 h. A low-magnification SEM image is shown in Fig. 2a, exhibiting that the as-synthesized product is relatively regular and uniform CdS nanoparticles. These nanoparticles have good monodispersity. The high-magnification SEM image



**Fig. 1** XRD patterns of the resultant products obtained at different reaction times by hydrothermal reaction of TAA and  $\text{Cd}(\text{NO}_3)_2 \cdot 4\text{H}_2\text{O}$  with 1.00 g of PVP at  $180^\circ\text{C}$ : (a) 0.5 h, (b) 1.5 h, (c) 4 h, (d) 8 h



**Fig. 2** **a, b** SEM; **c** EDS; and **d** TEM images of the resultant product obtained by hydrothermal reaction of TAA and  $\text{Cd}(\text{NO}_3)_2 \cdot 4\text{H}_2\text{O}$  with 1.00 g PVP at 180 °C for 8 h

in Fig. 2b confirms that the product is flower-like CdS nanostructures with the average diameter of 150 nm. EDS analysis in Fig. 2c demonstrates that the crystal consists of Cd and S elements. Moreover, according to the quantitative analysis of EDS, the Cd:S molar ratio is about 1: 0.96, which is consistent with stoichiometric CdS. Figure 2d illustrates the typical TEM image of an individual CdS nanoparticle, and it is interesting that the nanoparticle is ring structure but not solid structure. The strong contrast between the dark edge and pale center is the evidence for its ring structure.

During the formation process of CdS nanorings with flower-like morphology, comparative experiments were carried out to explore the influence of PVP. The amount of PVP was different from the former and other experimental conditions were kept unchanged. When PVP is absent, the product is composed of irregular CdS nanoparticles of which diameter ranges from 30 to 200 nm, which can be seen in Fig. 3a. When the content of PVP is increased to 0.10 g, the product is aggregates

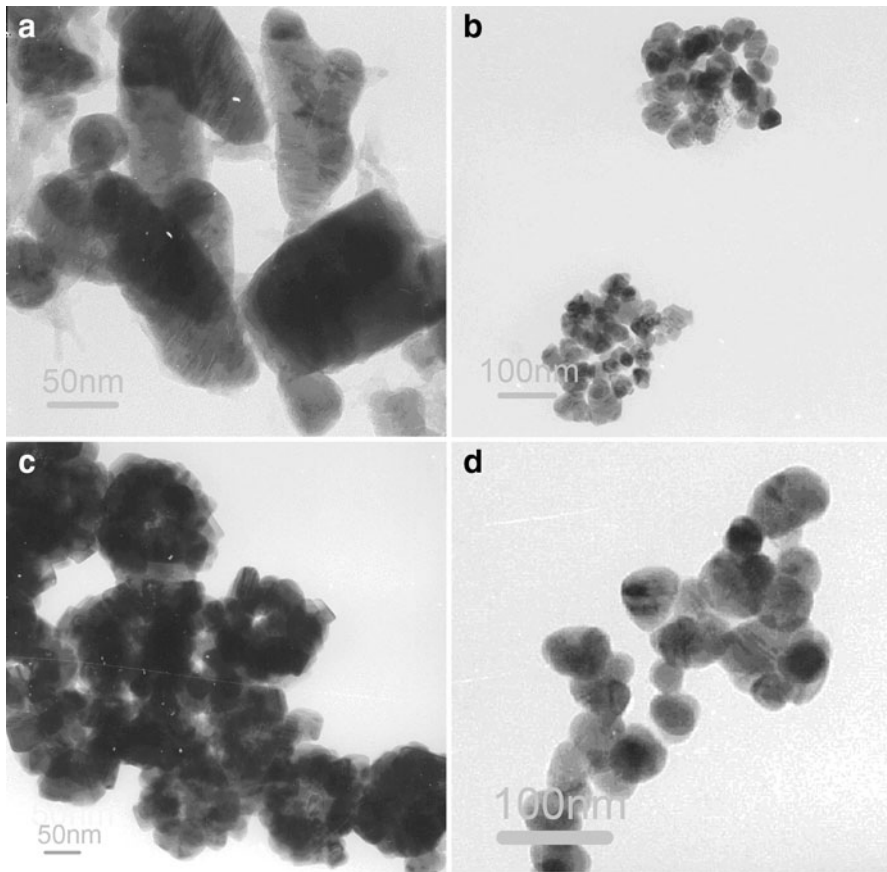


**Fig. 3** TEM images of CdS synthesized at 180 °C for 8 h with different amounts of PVP: **a** 0.00 g, **b** 0.10 g, **c** 0.50 g, **d** 5.0 g

composed of nanoparticles, and the average diameter of these aggregates is about 200 nm, which could be seen in Fig. 3b. Figure 3c shows TEM image of the sample prepared with 0.50 g PVP. Nanorings were observed, however, the ring structure is imperfect. The evidence is that the contrast between edge and center is not obvious. Even more interesting result is that the product prepared by 5.00 g PVP is nanoparticles with the diameter ranges from 30 to 50 nm but not nanorings, as is shown in Fig. 3d. This indicates that the formation of these novel flower-like CdS nanorings may be dependent on right amount of PVP. Specifically, if the amount of PVP is lower than 0.50 g or higher than 5 g, products are not nanorings but aggregates or nanoparticles. Therefore, the presence of the PVP is a key factor for influencing the growth of the flower-like CdS nanorings.

In order to understand the growth mechanism of CdS nanorings with flower-like morphology accurately, time-resolved experiments were carried out. The TEM images of the as-prepared samples collected at different stages are illustrated in

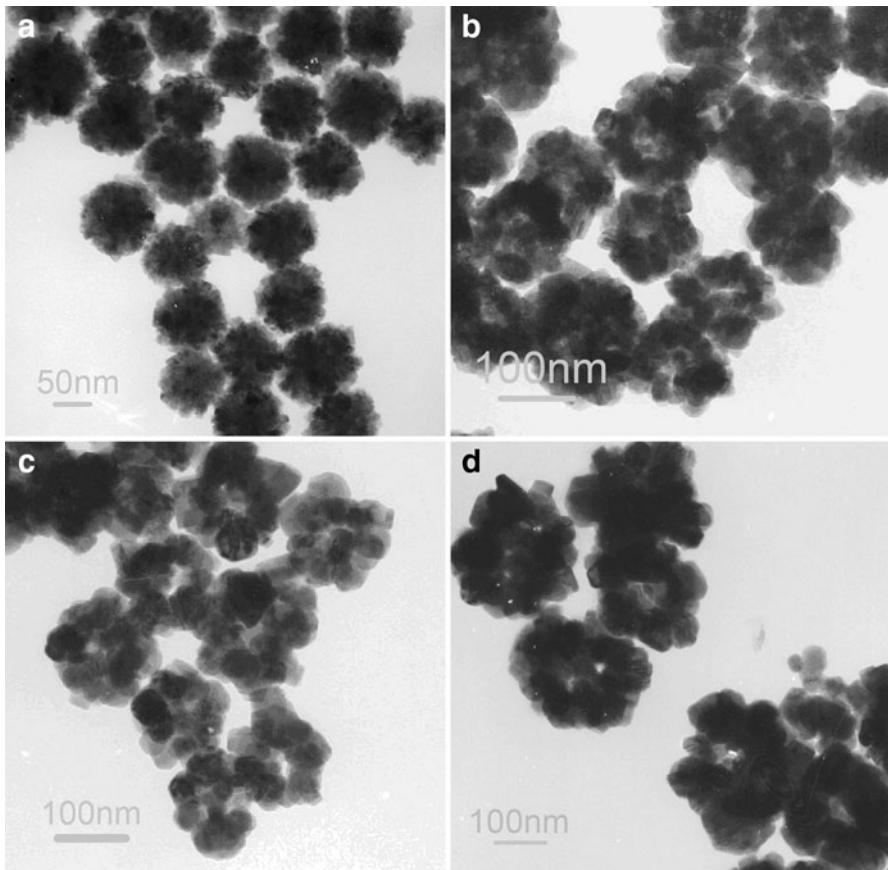
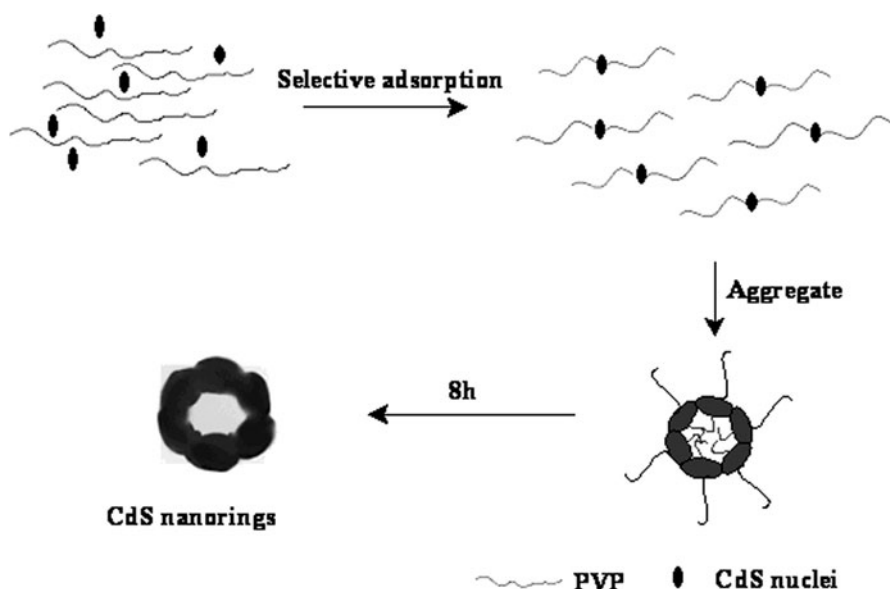


**Fig. 4** TEM images of the samples obtained from a series of parallel reactions for different durations: **a** 0.5 h, **b** 1.5 h, **c** 4 h, **d** 12 h

Fig. 4, depicting the formation process of CdS nanorings clearly. The sample after 0.5 h reaction in Fig. 4a consists of well-defined nanospheres by 70 nm average diameter. That illustrates the nanoring organization starting from 0D building blocks. Figure 4b displays the TEM image of the sample after reacting for 1.5 h. Nanorings are initially formed, but the structure of the ring is imperfect. As the reaction time increased, perfect nanorings are gradually formed (Figs. 2d, 4c). With a reaction time up to 8 h, a beautiful CdS nanoring is observed in Fig. 2d. Furthermore, to prolong time to 12 h (Fig. 4d), the ring structure is stably maintained, but the size of nanoring is increased from 150 to 200 nm.

On the basis of the time-dependent experiments we speculate the possible formation process of the sample. When PVP is added into  $\text{Cd}(\text{NO}_3)_2 \cdot 4\text{H}_2\text{O}$  solution, the free  $\text{Cd}^{2+}$  can coordinate bonding with oxygen atoms at PVP chains to form the PVP- $\text{Cd}^{2+}$  complex, and then the attack of  $\text{S}^{2-}$  causes the formation of initial CdS nuclei [13]. Simultaneously, as a modifier, the macromolecule PVP possibly adsorbs



**Scheme 1** Proposed growth process for the formation of CdS nanorings with flower-like morphology

onto some planes of the incipient CdS nuclei. However, other facets which are not covered by PVP may aggregate together, and the incipient CdS nanorings could be formed, which is shown in Fig. 4b. With the prolongation of reaction time, regular and uniform nanorings are obtained, accompanying an Ostwald ripening process (Fig. 2d). That is to say, PVP has two important roles: preventing the aggregation of CdS nucleus in the initial nucleation stage through coordination with  $\text{Cd}^{2+}$  and kinetically controlling the growth of some facets [13]. The possible growth process is schematically illustrated in Scheme 1.

Notably, when the reaction is conducted with the absence of PVP or small amounts PVP, there are lots of uncovered facets of the incipient CdS nuclei, and irregular particulates or aggregates (Fig. 3a, b) will be obtained. What is more, when there are not uncovered facets, aggregation will gradually cease. In that case, nanoparticles are obtained but not nanorings (Fig. 3d). As mentioned above, if the amount of PVP is lower than 0.5 g or higher than 5 g, nanorings will not finally be obtained, indicating that the macromolecule PVP dominates the whole growth process.

We also carried out basal optical property examination to evaluate the quality of the products. Figure 5 shows the room-temperature UV–vis spectra of irregular CdS nanoparticles (Figs. 3a, 5a) and nanorings with flower-like morphology (Figs. 2, 5b). The absorption peak appears at 523 nm in Fig. 5b while there is considerable red-shift compared to that of Fig. 5a, which is probably due to the relationship between the product surface state and its optical properties [20]. To be specific, surface defects of CdS nanorings reduced after the modification of PVP macromolecules.



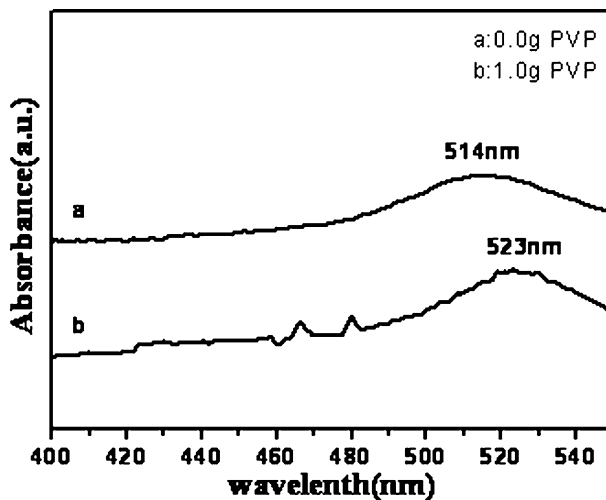


**Fig. 5** UV–vis absorption spectra of CdS nanomaterials obtained by hydrothermal reaction of TAA and  $\text{Cd}(\text{NO}_3)_2 \cdot 4\text{H}_2\text{O}$  with (a) 0.00 g, (b) 1.00 g PVP at 180 °C for 8 h

## Conclusions

Well-defined CdS nanorings with flower-like morphology have been successfully synthesized by hydrothermal reaction of  $\text{Cd}(\text{NO}_3)_2 \cdot 4\text{H}_2\text{O}$  and TAA with PVP as capping agent at 180 °C for 8 h. The amount of PVP and the reaction time are the important factors in the fabrication of CdS nanorings. On the basis of these experiments, the possible growth mechanism of the CdS nanorings with flower-like morphology is put forward. This facile approach is expected to be extended to fabricate other novel 3D nanostructures by selecting appropriate capping agent. The absorption peak of CdS nanorings is red-shifted to 523 nm in the UV–vis absorption spectrum.

**Acknowledgments** This work was financially supported by the National Natural Science Foundation of China (No. 50903045) and the Provincial Natural Science Foundation (No. Z2005F03).

## References

1. Wang D, Li D, Guo L et al (2009) Template-free hydrothermal synthesis of novel three-dimensional dendritic CdS nanoarchitectures. *J Phys Chem C* 113:5984–5990
2. Chen M, Kim YN, Li C et al (2008) Controlled synthesis of hyper-branched cadmium sulfide micro/nanocrystals. *Cryst Growth Des* 8(2):629–634
3. Mondal SP, Dhar A, Ray SK (2007) Optical properties of CdS nanowires prepared by dc electrochemical deposition in porous alumina template. *Mater Sci Semiconduct Process* 10:185–193
4. Banerjee R, Jayakrishnan R, Ayyub P (2000) Effect of the size-induced structural transformation on the band gap in CdS nanoparticles. *J Phys: Condens Matter* 12:10647
5. Seoudi R, Shabaka A, Eisa WH et al (2010) Effect of the prepared temperature on the size of CdS and ZnS nanoparticles. *Phys B* 405:919–924



6. Zhang WH, Shi JL, Chen HR et al (2001) Synthesis and characterization of nanosized ZnS confined in ordered mesoporous silica. *Chem Mater* 13:648–654
7. Zhang H, Liu G, Wan X et al (2009) Synthesis and characterization of single-crystalline CdS nanorods prepared by  $\gamma$ -irradiation. *J Mater Res* 24:227–236
8. Wang Y, Tang Z, Kotov NA (2005) Bioapplication of nanosemiconductors. *Mater Today* 8:20–31
9. Puangmali T, Califano M, Harrison P (2008) Interband and intraband optical transitions in InAs nanocrystal quantum dots: a pseudopotential approach. *Phys Rev B* 78(24):1–10
10. Balberg I (2009) Electrical transport mechanisms in ensembles of silicon quantum dots. *Phys Status Solidi C* 5:3771–3775
11. Jing M, Gai H, Wang Z (2010) Poly (vinyl alcohol)-assisted solvothermal growth of CdS dumbbells and necklaces. *Polym Bull* 64:413–419
12. Cao HQ, Wang GZ, Zhang SC et al (2006) Growth and optical properties of wurtzite-type CdS nanocrystals. *Inorg Chem* 45:5103–5108
13. Fan L, Guo R (2009) Controlled synthesis of pyramid-aggregated sphere-like cadmium sulfide in the presence of a polymer. *Cryst Growth Des* 9(4):1677–1682
14. Dongre JK, Ramrakhiani M (2009) Synthesis of flower-like CdS nanostructured films and their application in photoelectrochemical solar cells. *J Alloys Compd* 487:653–658
15. Nan YX, Chen F, Yang LG, Chen HZ (2010) Electrochemical synthesis and charge transport properties of CdS nanocrystalline thin films with coniferlike structure. *J Phys Chem C* 114:11911–11917
16. Chen F, Zhou R, Yang L et al (2008) Large-scale and shape-controlled syntheses of three-dimensional CdS nanocrystals with flowerlike structure. *J Phys Chem C* 112:1001–1007
17. Xiong S, Xi B, Qian Y (2010) CdS hierarchical nanostructures with tunable morphologies: preparation and photocatalytic properties. *J Phys Chem C* 114:14029–14035
18. Tong H, Zhu YJ (2006) Synthesis of CdS nanocrystals based on low-temperature thermolysis of one single-source organometallic precursor. *Nanotechnology* 17:845–851
19. Bandarnayake RJ, Wen GW, Lin JY et al (1995) Structural phase behavior in II–IV semiconductor nanoparticles. *Appl Phys Lett* 67:831–833
20. Lin Y, Zhang J, Sargent EH et al (2002) Photonic pseudo-gap-based modification of photoluminescence from CdS nanocrystal satellites around polymer microspheres in a photonic crystal. *Appl Phys Lett* 81(17):3134–3136